Experimentation and Simulation of the Combustion of Biomass Briquettes in Southern China

Bo Lou,[a,*] Sike Wu,[a] Xiaocong Wang,[b] Kuo Ma,[b] and Maodong Li [b]

The thermogravimetry (TG) of typical biomass briquettes used as fuel in southern China was analysed to investigate the influences of fuel grain size and heating rate on combustion. The results suggested that grain size and heating rate exerted little influence on combustion. In accordance with the data and the TG results obtained from the fuel, a biomass grate incinerator process was numerically simulated using fluid dynamics-based incinerator code (FLIC) software to obtain the solid phase temperature distribution of the fuel along the bed length, the spatial temperature distribution of flue gas, and the underlying variation laws of the primary components. A comparison of the mass-loss curves from the numerical simulation to the TG analysis demonstrated that the two curves exhibited consistently staged variations, including dehydration and drying, fast pyrolysis and combustion of volatiles, and the burnout of residual carbon. The specific characteristics of the fuel obtained from these tests improved the accuracy of the numerical simulation, while the variations in temperature and components obtained were conducive to optimising the combustion process of a biomass incinerator.

Keywords: Biomass; Grate incinerator; Numerical simulation; Thermogravimetric analysis

*Contact information: a: School of Electric Power, South China University of Technology, Guangzhou, 510640, P.R. China; b: Guangzhou Special Pressure Equipment Inspection and Research Institute, Guangzhou, 510663, P.R. China; *Corresponding author: loubo@scut.edu.cn*

INTRODUCTION

Owing to environmental problems caused by fossil fuels, and the rising prices and gradually exhausting sources, biomass energy, as a green and renewable energy, has increasingly become the focus of research and socio-political attention (van Dam *et al.* 2008). Biomass is composed of compounds resulting from photosynthetic processes (Bridgwater 2012) and is a substitute to fossil fuels for both heating and electricity generation (Luque *et al.* 2008). Biomass has few energy storage problems in comparison with other renewable energy such as wind and solar, and it is widely available in most countries and ranks as the fourth source of energy in the world, occupying roughly 14% of world final energy consumption (Saidur *et al.* 2011).

Biomass briquettes are made from agricultural and forestry waste. As a densified product, biomass briquettes benefit from an increased energy density and a convenient shape, typically cylindrical or octagonal. Such briquettes reduce the costs and problems associated with transport and storage of biomass (Roy *et al*. 2012). Biomass combustion is one of the main conversion routes for make use of biomass energy (Yin *et al*. 2008). The biomass combustion method is characterised by net zero CO_2 emissions (Pedersen *et al*. 1996), as well as reduced by-production of SO_2 and NO_x (Qiu 2013). Grate firing is the most common technique in small- to medium-sized heating and industrial units (Van and Koppejan 2007). In these boilers, the fuel is introduced at one end of the grate and

transported to the other end, while the primary air is supplied from underneath the grate (Sefidari *et al*. 2014).

Magdziarz and Wilk (2013) investigated the thermogravimetry (TG) of pelletized wood fuel and oat straw by obtaining such variables as the starting and ending temperatures of their combustion and the maximum reaction rate temperature of these two biomass fuels. H_2O was the main product formed for all the East Asian biomass samples studied by Aghamohammadi *et al*. (2011); gaseous products such as CO, H_2O, CO_2, CH_4, and COOH+ were found in the TG-MS test. The results of five different experiments (SEM, PSD, EDX, TG, and DTG) for six biomass samples and their wastes were analyzed by Fernández *et al*. (2012), and the almond shell was found to be the most suitable for thermal conversion in chambers.

Compared with experimentation, computer simulation is a relative costless and convenient way to get a clear perspective of the flow and combustion phenomena within an entire combustion system, and it could be used as a design and analysis tool to improve the overall performance, such as to augment efficiency and to reduce pollution (Porteiro *et al.* 2009). A kinetic model based on a multi-component, multi-phase, and multi-scale system had been shown to provide a wide range of useful predictions in a feasible way (Ranzi *et al*. 2014). A one-dimensional model of a BioGrate furnace was developed to investigate the process phenomena in the furnace; the simulation results demonstrated the significant dependence of the combustion process on moisture content (Boriouchkine *et al*. 2012). A team used a software program called FLUENT to simulate the combustion of a biomass packed bed. The results showed that an increase in airflow shortened the burnout time (Gómez *et al*. 2014). The Finite Element code XENIOS++ was used for implementing a comprehensive computational model for biomass combustion; by such an approach it was possible to predict the thermal field within both the solid and the gas phase (Venturini *et al*. 2010). When the fluid dynamics-based incinerator code (FLIC) software was applied to simulate the biomass combustion process, it was reported that this process was completed in three stages: ignition combustion, primary combustion, and fixed carbon combustion (Yang *et al.* 2004). Most of the fuel was burnt inside the furnace and little CO was released from the system due to the high flue gas temperature in the furnace. The use of wood heating system resulted in much lower CO_2 emissions than from a fossil fuel, according to a study combining FLIC and FLUENT (Zhang *et al*. 2010). The combustion characteristics of a direct straw combustion incinerator operating at 200 t/d were investigated under varied conditions, *i.e*., with controlled variations in the volume ratios of primary and secondary inlet airflow as simulated by FLIC and FLUENT (Yu and Ma 2008). These previous studies provided the basis for the present study.

In southern China, the combustion of biomass briquettes has not yet been investigated by means of combined thermal analysis and numerical simulation, and the combustion system is not yet sufficiently understood. Besides, currently many small scale biomass boilers are modified from coal-fired boilers. The significant differences between coal and biomass result in low efficiency and less reliable burning condition. In order to make full utilization of biomass energy, it is imperative to improve the biomass boilers according to specific properties of biomass. This study first analysed the industrial characteristics, elemental compositions, and calorific value of typical biomass briquettes in southern China. Then, investigations were made into the combustion characteristics thereof using a TG analyser. Using the data obtained, the biomass grate incinerator was numerically simulated by means of FLIC software to obtain combustion parameters for the bed layer and incinerator, including the heat release rate, the compositions of solid phase

and gas phase, and the temperature profile along the bed length. The results obtained from the test and simulations were found to be conducive to further optimisation of the combustion process of biomass in incinerators and provided a reference for the design, construction, and optimal operation of biomass grate incinerators.

EXPERIMENTAL

The Structure of Biomass Grate Incinerators

This study used a biomass grate steam incinerator, located in a factory in southern China, which had a rate of evaporation capacity of approximately 2 t/h and a saturated steam temperature of 194 °C. Figure 1 shows the structure of the incinerator. The incinerator was 2.7 m long and 1.0 m wide. Air was blown into the incinerator from the bottom, while the hot flue gas flowed onto the heated surface from the space between the arch and the incinerator wall.

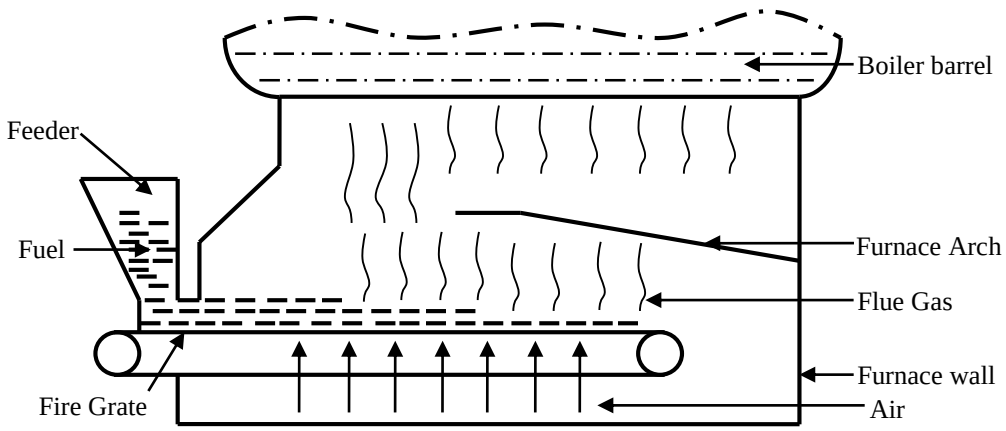

Fig. 1. Structure of a biomass grate incinerator

Materials

The fuel used in the incinerator was biomass in the form of briquettes, which had been compressed from typical biomasses available in southern China. The main components of the biomass included sawdust and sugarcane bagasse. Table 1 shows the ultimate, proximate, and LHV analyses.

Table 1. Ultimate and Proximate Analyses of the Samples

Ultimate Analysis(wt%, ar)				Proximate Analysis(wt%, ar)				LHV(kJ/kg)
C	H	N	O	FC	MC	VM	Ash	16663
48.71	5.28	0.10	45.91	17.29	3.77	72.74	6.20	

Methods

TG testing of the biomass briquette

As is shown in Fig. 2, a German NETZSCH STA409PC simultaneous thermal analyser was used for the TG testing, with pure nitrogen serving as its protective atmosphere (supplied at 20 mL/min). The test samples, namely, 7 to 8 mg-quantities of

biomass powder, were separated into their various component raw materials using 40-and 80-mesh square aperture sieves; heating rates were set to 20, 30, and 40 K/min; all the experiments were under the controlled atmosphere of nitrogen (79 mL/min) and oxygen (21 mL/min). The initial temperature, 313 K, was increased to a termination temperature of 1273 K. The reaction time, the change pattern of gravity, and temperature were recorded by the analyser. The TG testing process is illustrated in Figure 3.

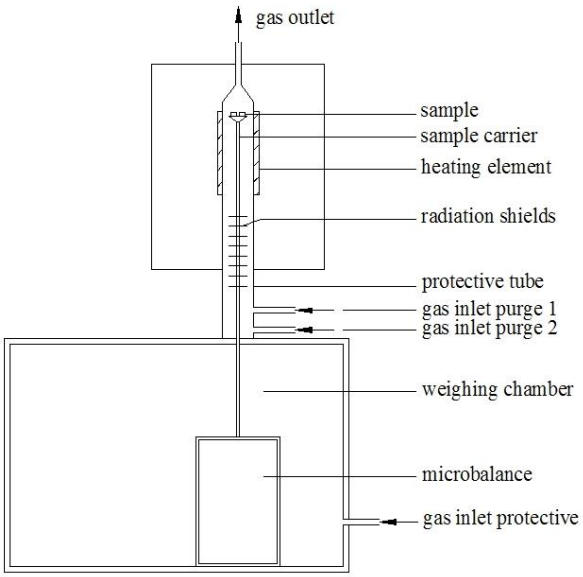

Fig. 2. The structure of thermal analyser

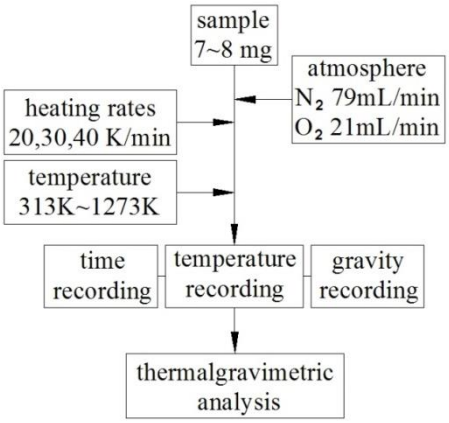

Fig. 3. The schematic diagram of thermogravimetric analysis

The FLIC combustion simulation

A fluid dynamics-based incinerator code, developed by Sheffield University's Waste Incineration Center in the UK, has been used mostly to simulate the combustion of solid waste through four processes (Yang *et al.* 2002; Ryu *et al.* 2004): water evaporation, volatile emission, volatile combustion, and char gasification. The bed is assumed as a movable porous medium which is divided into many cells. Relevant parameters (*e.g.* temperature, percentage of moisture, carbon, *etc*.) of cells are assumed to be uniform. The transport equations include the component transport and heat transfer equations of the gaseous phase, the motion and heat transfer equations used for solid particles, and the

radiation heat transfer equation applied to the bed (Yang *et al.* 2003). The characteristic length of the biomass briquette in this simulation is less than 30 mm, which can be roughly regarded as thermally thin. Thus, the need for a separate solution for temperature profile inside the particles is eliminated by the assumption (Yang *et al.* 2005).

Based on both elemental and heat balances, the composition of the volatile gases was assumed to be CO, H_2, and CO_2 in the study, with a purpose of simplify the calculation. As a consequence, the model may be not be as accurate as other models that consider more types of gaseous compounds. Volatile hydrocarbons are assumed to be a single product, $C_mH_nO_l$, which is oxidized to produce CO and H_2. The kinetic rate for $C_mH_nO_l$ oxidation, and CO and H_2 burning, has been proposed by previous researchers (Field 1969, Wakao and Kaguei 1982, Peters 1995).

Gradients of the gaseous temperature, concentrations, and velocity are assumed to be the second-type boundary, and the third-type boundary is assumed at both the bottom of the bed and the top surface for temperature (Yang *et al.* 2004). Based on the fourth-order Runge-Kutta method and the principles of mass and energy conservation (Girgis 2004), the following parameters were set: the volatile gases were assumed to be CO (30.32%), H_2 (53.11%), and CO_2 (16.57%); the fuel was ignited by means of a radiative heat transfer process, with a radiative coefficient of 0.8 and a temperature of 1273 K; the primary volumetric airflow was set to 33.24 m^3/min at a temperature of 373 K; the initial temperature of the fuel was 303 K; the bed moved at a speed of 4.5 m/h; the whole combustion process lasted 36 min; the initial fuel height was 200 mm; the fuel density was 552 kg/m^3. The initial bed porosity was 0.65 (Lin 2012).

RESULTS AND DISCUSSION

TG Testing

Figures 4 and 5 show the TG and differential thermo-gravimetric (DTG) curves of the samples of different grain sizes. The very small difference in the curves suggest that combustion was practically unaffected by grain size and that it would thus be feasible to process the biomass briquettes at a very low stacking density using the compression molding method.

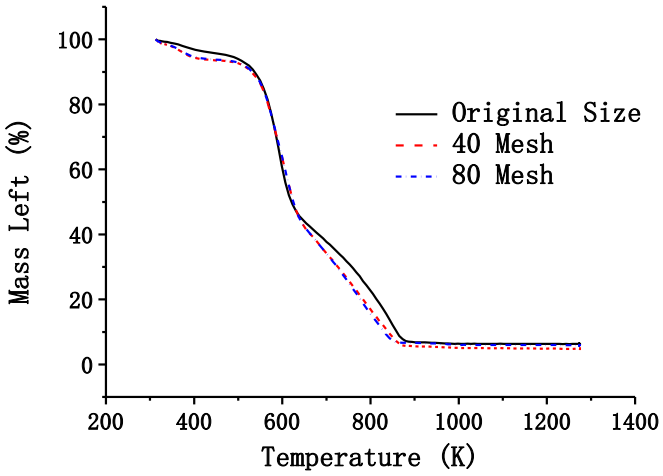

Fig. 4. The TG curves of samples with different grain sizes

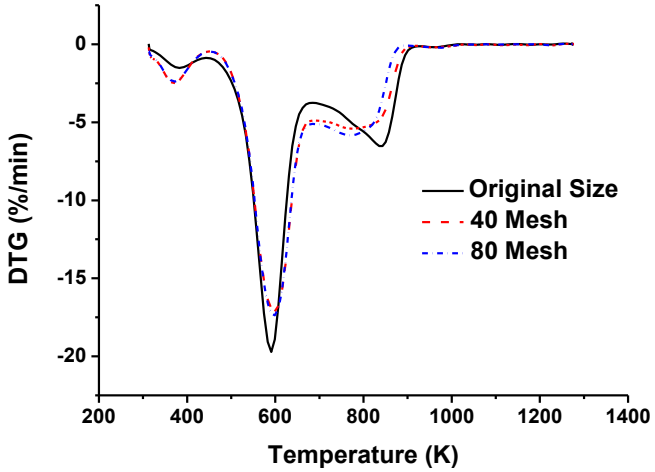

Fig. 5. The DTG curves of samples with different grain sizes

As the temperature was increased, the combustion of the biomass proceeded through three stages: dehydration and drying, fast pyrolysis and combustion of volatiles, and the burnout of residual carbon. The first two stages corresponded to the two mass-loss peaks on the DTG curves, while the last stage reflected the mass-loss during the residual carbon combustion process (Liao *et al.* 2013).

Figures 6 and 7 illustrate the TG and DTG curves at different heating rates, where the heating rate was inversely proportional to the percentage of residuals. The higher the heating rate, the lower the percentage of residuals. The reason for this relationship was that the heating rate of the fuel was lower than that of the environment, such that the characteristic combustion temperature increased and induced an overly high internal temperature in the ash. Some of the inorganic compounds in the ash that had not been extracted at this point reduced the residual content (Fang *et al.* 2012). The DTG curves showed that heating rate was proportional to the maximum mass loss rate.

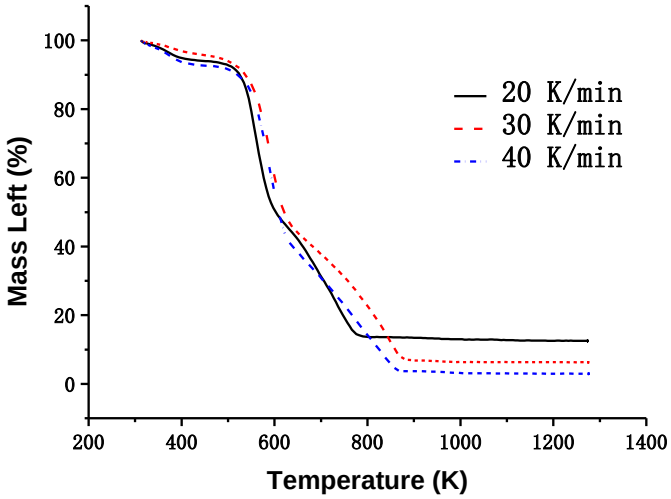

Fig. 6. TG curves at different heating rates

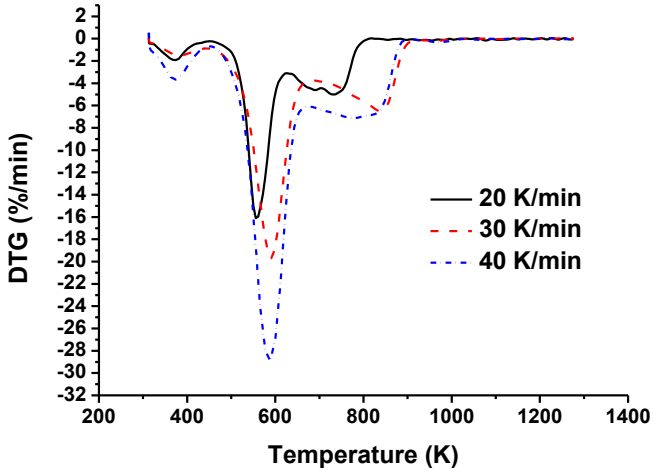

Fig. 7. The DTG curves at different heating rates

The Kissinger method was applied to obtain the dynamic equations that governed biomass combustion (Doyle 1961; Kissinger 1957). The pre-exponential factor and activation energy yielded were 5.2×10^6 and 110 kJ/mol, respectively, and these were used as input parameters for the reaction dynamic factors in the subsequent FLIC computational model.

Analysis of the Results of the Numerical Simulation

Figure 8 shows the temperature distribution in the solid phase. After entering the incinerator, the fuel was subjected to the radiative heat transfer of the flue gas and the convection of heat from the primary airflow on the bottom of the fire grate. As can be seen in Fig. 8, this process is reflected in the temperature increases at the bottom and top of the bed. When the fuel moved to approximately 0.5 m along the fire grate, the volatiles were emitted and then combusted under the applied heat. Meanwhile, the temperature of the bed surface increased rapidly to its maximum at 1360 K. This process constituted the main heat release stage of the overall combustion process. When the fuel moved to 1.4 m along the bed, the emission of volatiles gradually decreased. The fixed carbon combustion became the primary heat release source in the ensuing stage.

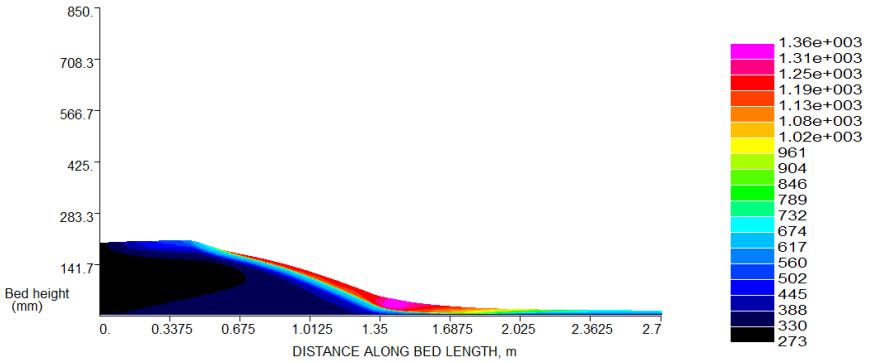

Fig. 8. Temperature distribution in the solid phase

Figures 9 through 11 show the variation in the main components of the biomass fuel. Figure 9 shows the variation in water content of the fuel. Because of the radiative heat transfer that occurred in the upper part of the bed and the convective heat transfer from the primary airflow occurring at the bottom of the bed, the water gradually evaporated from the biomass fuel in the form of a parabola-like distribution with respect to the height. Figure 10 shows the characteristics of the high volatile content (72.74%), while Fig. 8 demonstrates that when the surface temperature of the fuel exceeded 600 K, volatiles were emitted and combusted, followed by a reduction in combustion volume and a significant decrease in bed height. Figure 11 shows the variation in fixed carbon content. Although the ignition temperature was high, the amount of fixed carbon remained constant in the initial stage of combustion. While the fuels were being irradiated by flue gas and the combustion heat transfer of fuel was occurring, the fixed carbon began its slow combustion in two markedly different stages. The first stage saw the emission of a large amount of volatiles, and the fixed carbon content increased from the original 17.29% to approximately 76%. The second stage involved the combustion of fixed carbon in the region from 1.4 to 2.4 m along the bed, causing the fixed carbon content to fall from 76% to 4% and then lower.

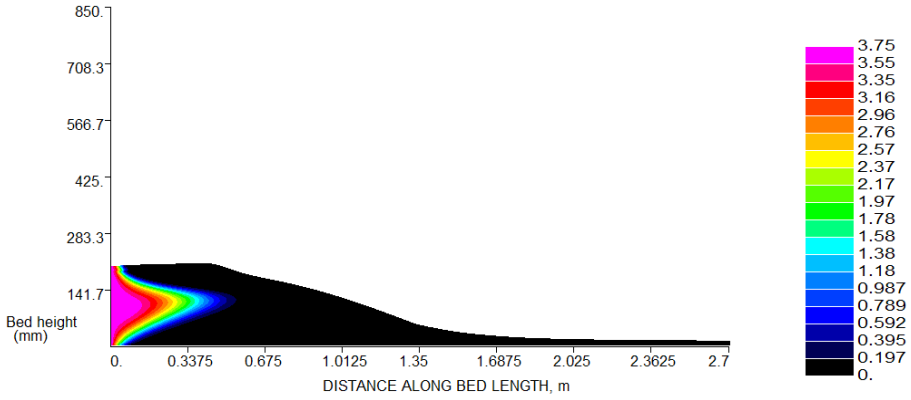

Fig. 9. Water content of the solid phase

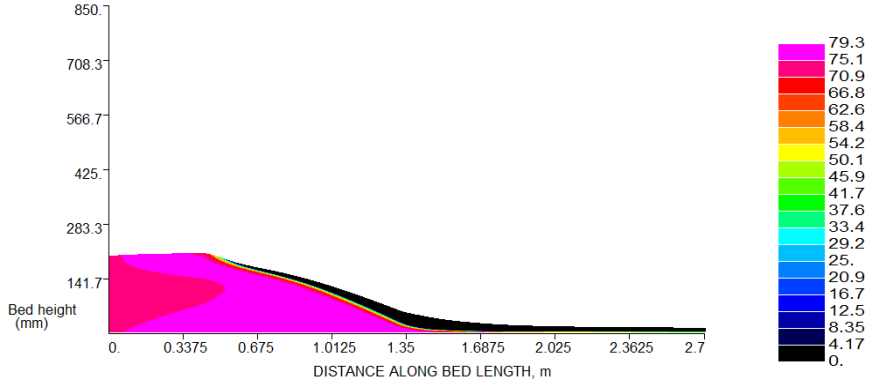

Fig. 10. Volatile content of the solid phase

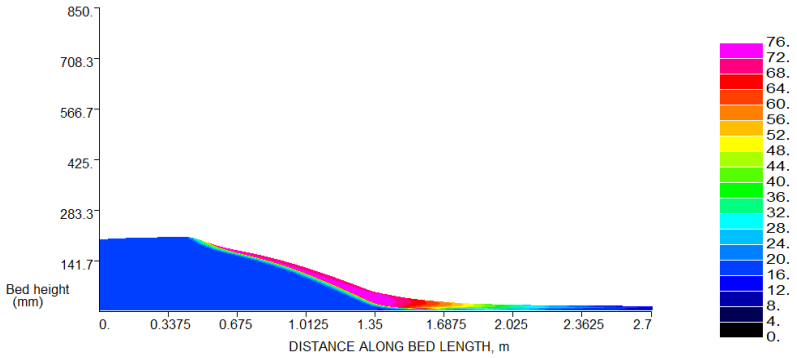

Fig. 11. Fixed carbon content of the solid phase

Figure 12 shows the temperature distribution in the flue gas. The release of heat mainly occurred during the combustion of the volatiles and fixed carbon. With the emission and combustion of volatiles, the flue gas in the incinerator underwent a rapid temperature increase. The section from 0.5 to 1.7 m in Fig. 12 shows the highest temperature, 1100 to 1670 K. For this reason, in future incinerator designs, the whole high-temperature section should be completely covered by the arch to concentrate the radiation of the flue gas onto the bed and accelerate the rate of water evaporation from the fuel.

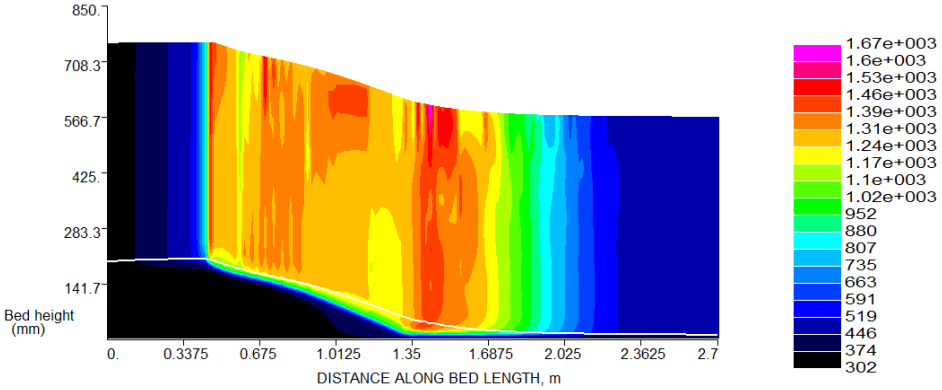

Fig. 12. Temperature distribution in the flue gas

Figure 13 shows variation rates of components comprising the biomass briquette.

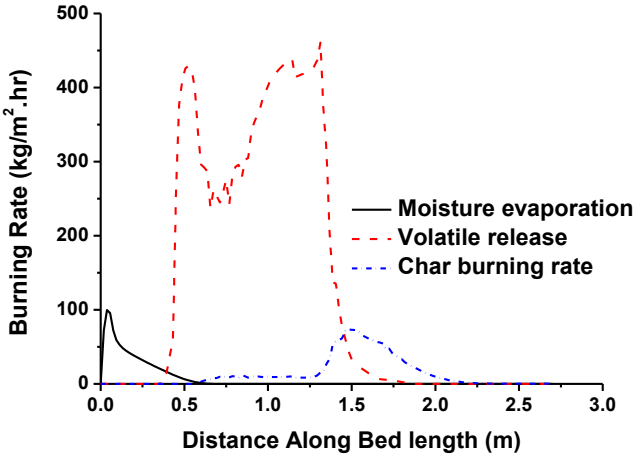

Fig. 13. Variation rates of the components in the fuel

Figure 14 shows the mass faction variations of the components in the flue gas. Values correspond to integral results. The section from 0 to 0.5 m corresponded to the main water evaporation stage, which had a water vapor mass fraction of 10%. From 0.5 m onward, volatiles were separated out as the temperature rose to 600 K; the gases emitted included CO and H_2. Meanwhile, combustible O_2 was rapidly consumed (with an O_2 content reduction from 21% to 0%), yielding CO_2 and H_2O. Due to its higher temperature requirement, the fixed carbon combustion was not observed until the bed surface temperature reached 973 K at 0.6 m, whereupon it yielded CO_2. At 1.5 m, the combustion rate was maximised, as was the temperature, at 1360 K. At 2.2 m, the fixed carbon had achieved burnout, which was followed by a reduction in bed surface temperature to 700 K. The oxygen was then gradually consumed, with a mass fraction of approximately 21%.

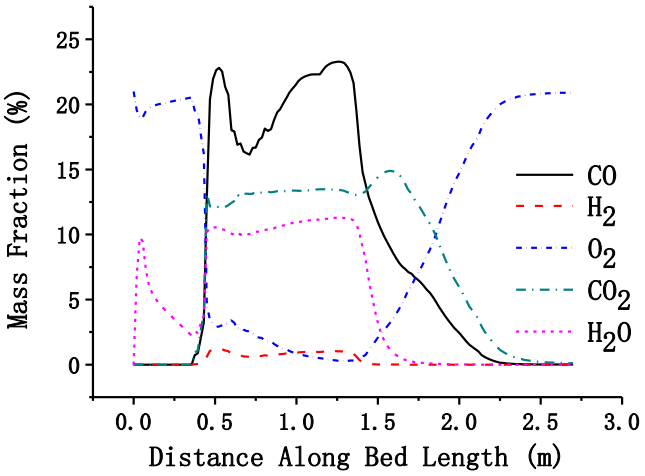

Fig. 14. The mass faction variations of the components in the flue gas

To improve the efficiency of biomass briquette burning and mitigate the influence of poor air distribution on the combustion process, several stages of combustion, which differed based on their air supply, were introduced during the actual operation of the biomass incinerator. For example, in the sections from 0 to 0.3 m and 2.2 to 2.7 m, the air supply was decreased to approximately 10 to 20% of the overall air supply for the process, on the basis of the consideration that the evaporation of water and the combustion of residual carbon did not need oxygen, or only needed a small amount of oxygen, in order to take place. The small amount of air supply in this section was mainly used to promote the flow of flue gas above the bed. The section from 0.3 to 2.2 m, meanwhile, corresponded to the combustion stage of the volatiles and fixed carbon in the biomass. Thus, the air supply in this section was increased to 80 to 90% of the total supplied air in order to improve the fuel combustion rate (by enriching the mixture of combustible components via increased oxygen) as well as to avoid heat loss from the flue gas that could occur due to excess air supply in the incinerator.

Combination of Numerical Simulation and TG Test Combustion Analyses

Figures 15 and 16 show the TG and DTG curves obtained by the FLIC simulation and TG analysis, respectively (the horizontal axis is time). It can be seen that the two curves were consistent with regard to overall trend. The first instance of variation was found in the water evaporation section. As the temperature increased, the emission and combustion

of volatiles triggered a decrease in the amount of residual solids. After the combustion of the volatiles, the fixed carbon was combusted and achieved burnout. However, due to the differences in the heating conditions, the combustion in the incinerator differed from that in the TG test. This was attributed to the fact that, in the grate incinerator, the heat transfer was faster due to the higher degree of flue gas radiation that occurred in the larger space. In contrast, since the temperature in the TG test increased uniformly, the duration of the water evaporation stage during the initial stage was significantly shorter in the case of the grate incinerator than in that of the TG test. Hence, the FLIC numerical simulation yielded a larger water evaporation peak. Secondly, in the volatile emission stage, the FLIC numerical simulation produced a lower slope for the mass-loss curve and a far smaller mass-loss peak for the DTG curve than did those in the TG test due to the influence of bed thickness.

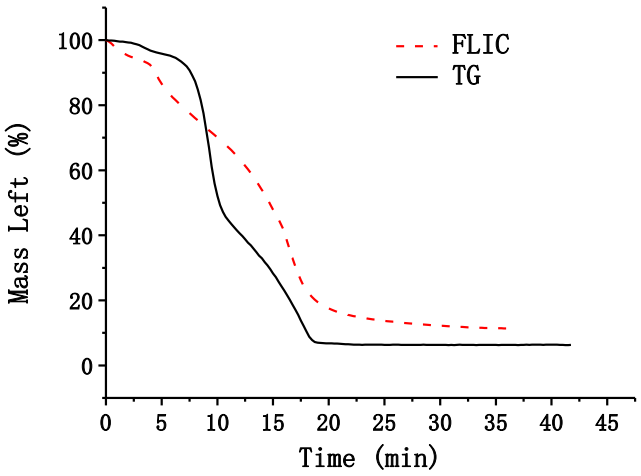

Fig. 15. Comparison of the TG curves obtained in theFLIC simulation and in the TG analysis

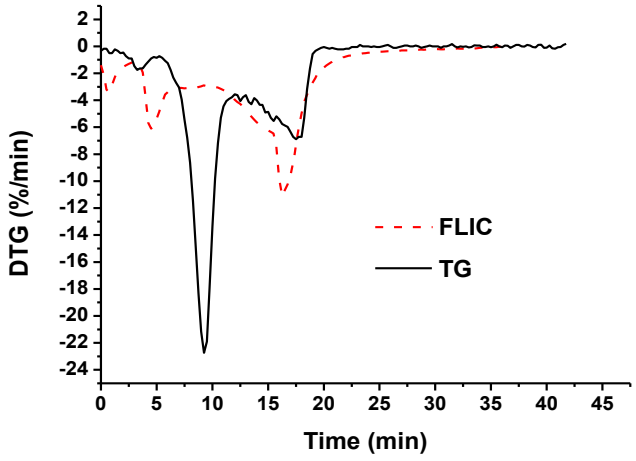

Fig. 16. Comparison of DTG curves, curves obtained in FLIC simulation, and the curves from TG analysis

As heat was transferred from the bed surface to the middle and bottom sections, the emission of volatiles that occurred at the bottom and middle sections lasted longer. In

addition, the temperature in the TG test was uniformly increased from 40 K to 1273 K. When the temperature rose to 1000 K and above, the volatiles and fixed carbon burned simultaneously. On the mass-loss curve, this process was presented as the insignificant combustion stage of the fixed carbon. However, in the grate incinerator, the curve for the slow combustion of the fixed carbon was more obvious because the temperature was reduced in the burnout stage of the fixed carbon. As a result of structure and combustion conditions differences, the combustion efficiency of grate incinerator was lower than for the TG test, and an 11% residual mass fraction was found, which was larger than the 6% yielded by the TG test. Therefore, in the future, the combustion process should be optimised using numerical simulation.

CONCLUSIONS

1. The variables heating rate and grain size exerted little influence on the combustion of the biomass briquette. It was feasible to treat the biomass briquette with extremely low-density packing using a compression molding method. The pre-exponential factor and the activation energy of the biomass briquette, obtained from the dynamics analysis, were 5.2×10^6 and 110 kJ/mol, respectively.
2. The combustion process was completed in three stages: water evaporation (0 to 0.5 m), emission and combustion of volatiles (0.3 to 1.7 m), and fixed carbon combustion (0.6 to 2.2 m). The water content in the fuel exhibited a parabola-like distribution with respect to the height. After the emission of volatiles, the bed height was significantly reduced. When the volatiles had been fully emitted, the fixed carbon content increased from 17.29% to approximately 76%, and then dropped to 4% in the ensuing combustion.
3. The flue gas distribution could be obtained by means of FLIC simulation. The section from 0.5 to 1.7 m corresponded to the high temperature region, which had a temperature of 1100 to 1670 K. In the design of future biomass incinerators, the whole high-temperature region should be covered by the arch to intensify the radiation of the flue gas onto the bed.
4. The mass-loss curves obtained by the TG test and the numerical simulation showed identical trends. However, because of the differences in heating conditions, the numerical simulation differed from the TG test in several other respects, *e.g.*, a lower water-loss peak and a higher volatile emission mass-loss peak arose in the TG test.

ACKNOWLEDGMENTS

The authors are grateful for the support of the Guangzhou Bureau of Quality and Technical Supervision (HT13050327), the Key Laboratory of Efficient and Clean Energy Utilisation of Guangdong Institutes (KLB10004), and the Guangdong Natural Science Foundation (S2013010016748).

REFERENCES CITED

Aghamohammadi, N., Nik Sulaiman, N. M., and Aroua, M. K. (2011). "Combustion characteristics of biomass in SouthEast Asia," *Biomass Bioenergy* 9(35), 3884-3890.

Boriouchkine, A., Zakharov, A., and Jamsa, S. L. (2012). "Dynamic modeling of combustion in a BioGrate furnace: The effect of operation parameters on biomass firing," *Chemical Engineering Science* 1(69), 669-678.

Bridgwater, A.V. (2012). "Review of fast pyrolysis of biomass and product upgrading," *Biomass and Bioenergy* 38, 68-94.

Doyle, C. D. (1961). "Kinetic analysis of thermogravimetric data," *Journal of Applied Polymer Science* 5(15), 285-292.

Fang, X., Jia, L., Tan, Z. T., and Wang, Z. M. (2012). "Effect of oxygen, moisture content and heating rate on biomass combustion," *Journal of Beijing Jiaotong University* 36(1), 145-149.

Field, M. (1969). "Rate of combustion of size-graded fractions of char from a low rank coal between 1200 and 2000 K," *Combust Flame* 13, 237-252.

Fernández, R. G., García, C. P., Lavín, A. G., de Las Heras, B., and Julio, L. (2012). "Study of main combustion characteristics for biomass fuels used in boilers," *Fuel Processing Technology*, 103, 16-26.

Girgis, E. (2004). *Fuel Devolatilization in Packed Bed Wood Combustion*, Masters thesis, University of Ottawa.

Gómez, M. A., Porteiro, J., Patiño, D., and Miguez, J. L. (2014). "CFD modelling of thermal conversion and packed bed compaction in biomass combustion," *Fuel* 117(Part A), 716-732.

Kissinger, H. E. (1957). "Reaction kinetics in differential thermal analysis," *Analytical Chemistry* 11(29), 1702-1706.

Liao, Y. F., Zeng, C. C., and Ma, X. Q. (2013). "Thermogravimetric analysis of pyrolysis and combustion characteristics of typical biomass in South China," *Journal of South China University of Technology (Natural Science Edition)* 41(8), 1-8.

Lin, H. (2012). *Operation Optimization of Municipal Solid Waste Incinerator Based on CFD and Emission Characteristics Study by Experiment*, Masters thesis, South China University of Technology.

Luque, R., Davila, H., Campelo, J., and Clark, J. (2008). "Biofuels: A technological perspective," *Energy Environ. Sci.* 5(1), 542-564.

Magdziarz, A., and Wilk, M. (2013). "Thermogravimetric study of biomass, sewage sludge and coal combustion," *Journal of Energy Conversion and Management* 75, 425-430.

Pedersen, L. S., Nielsen, H. P., Kiil, S. R., Hansen, L. A., and Dam-Johansen, K., Kildsig, F., Christensen, J., and Jespersen, P. (1996). "Full-scale co-firing of straw and coal," *Fuel* 13(75), 1584-1590.

Peters, B. (1995). "A detailed model for devolatilization and combustion of waste material in packed beds," *Proceedings of the Third European Conference on Industrial Furnaces and Boilers (INFUB)*, Lisbon.

Porteiro, J., Collazo, J., Patin O, D., Granada, E., Moran Gonzalez, J.C., and Mi Guez, J. L. S. (2009). "Numerical modeling of a biomass pellet domestic boiler," *Energy & Fuels* 2(23), 1067-1075.

Qiu, G. Q. (2013). "Testing of flue gas emissions of a biomass pellet boiler and abatement of particle emissions," *Journal of Renewable Energy* 50, 94-102.

Ranzi, E., Corbetta, M., Manenti, F., and Pierucci, S. (2014). "Kinetic modeling of the thermal degradation and combustion of biomass," *Chemical Engineering Science* 110, 2-12.

Roy, Mohon, M., and Corscadden (2012). "An experimental study of combustion and emissions of biomass briquettes in a domestic wood stove," *Applied Energy* 99, 206-212.

Ryu, C., Yang, Y. B., Nasserzadeh, V., and Swithenbank, J. (2004). "Thermal reaction modeling of a large municipal solid waste incinerator," *Combustion Science and Technology* 176(11), 1891-1907.

Saidur, R., Abdelaziz, E.A., Demirbas, A., Hossain, M.S., and Mekhilef, S. (2011). "A review on biomass as a fuel for boilers," *Renewable and Sustainable Energy Reviews* 5(15), 2262-2289.

Sefidari, H., Razmjoo, N., and Strand, M. (2014). "An experimental study of combustion and emissions of two types of woody biomass in a 12-MW reciprocating-grate boiler," *Fuel* 135, 120-129.

van Dam, J., Junginger, M., Faaij, A., Jürgens, I., Best, G., and Fritsche, U. (2008). "Overview of recent developments in sustainable biomass certification," *Biomass and Bioenergy* 32(8), 749-780.

Van, L.S., and Koppejan, J. (2007). *The Handbook of Biomass Combustion and Co-firing*, Earthscan LLC, London.

Yin, C., Rosendahl, L.A., and Kær, S. K. (2008). "Grate-firing of biomass for heat and power production," *Progress in Energy and Combustion Science* 6(34), 725-754.

Venturini, P., Borello, D., Iossa, C., Lentini, D., and Rispoli, F. (2010). "Modeling of multiphase combustion and deposit formation in a biomass-fed furnace," *Energy* 7(35), 3008-3021.

Wakao, N., and Kaguei, S. (1982). *Heat and Mass Transfer in Packed Beds*, Gordon & Breach, London.

Yang, Y. B., Goh, Y. R., Zakaria, R., Nasserzadeh, V., and Swithenbank, J. (2002). "Mathematical modelling of MSW incineration on a travelling bed," *Waste Management* 22(4), 369-380.

Yang, Y. B., Ryu, C., Khor, A., Yates, N. E., Sharifi, V. N., and Swithenbank, J. (2005). "Effect of fuel properties on biomass combustion. Part II. Modelling approach—Identification of the controlling factors," *Fuel* 16(84), 2116-2130.

Yang, Y. B., Sharifi, V. N., and Swithenbank, J. (2004). "Effect of air flow rate and fuel moisture on the burning behaviours of biomass and simulated municipal solid wastes in packed beds," *Fuel* 83(11-12), 1553-1562.

Yang, Y. B., Yamauchi, H., Nasserzadeh, V., and Swithenbank, J. (2003). "Effects of fuel devolatilisation on the combustion of wood chips and incineration of simulated municipal solid wastes in a packed bed," *Fuel* 82(18), 2205-2221.

Yu, Z. S., and Ma, X. Q. (2008). "Numerical simulation of combustion in a straw-fired boiler," *Transactions of the Chinese Society for Agricultural Machinery* 39(4), 73-77.

Zhang, X., Chen, Q., Bradford, R., Sharifi, V., and Swithenbank, J. (2010). "Experimental investigation and mathematical modelling of wood combustion in a moving grate boiler," *Fuel Processing Technology* 11(91), 1491-1499.

Article submitted: May 14, 2014; Peer review completed: June 24, 2014; Revised version received: Aug. 1, 2014; Accepted: Aug. 2, 2014; Published: August 6, 2014.